

Kinetics of microbial Fe(III) oxide reduction in freshwater wetland sediments

Eric E. Roden¹ and Robert G. Wetzel²

The University of Alabama, Department of Biological Sciences, Tuscaloosa, Alabama 35487-0206

Abstract

The kinetics of microbial amorphous Fe(III) oxide reduction was investigated in sediments from a freshwater wetland in north central Alabama, USA. Fe(III) oxide concentrations decreased exponentially with time during anaerobic incubation of sediment slurries and homogenized surface sediments. Rates of organic carbon mineralization ($\Sigma\text{CO}_2 + \text{CH}_4$ accumulation) did not change markedly during the course of Fe(III) oxide reduction, which indicated that the exponential decline in Fe(III) oxide concentration over time resulted primarily from Fe(III) limitation rather than a decrease in organic matter decay rate. Initial rates of Fe(III) oxide reduction were linearly correlated with initial Fe(III) oxide concentrations in experiments with mixtures of Fe(III)-rich and Fe(III)-depleted sediment slurries. Similar results were obtained in experiments with sediment from various depth intervals in the upper 3 cm of freshly collected cores. These findings provide explicit evidence that microbial Fe(III) oxide reduction rates are first order with respect to amorphous Fe(III) oxide concentration in the wetland sediment. The observed first-order relationship between Fe(III) oxide concentration and reduction rate is consistent with established models of surface area-controlled mineral transformation. An experiment in which Fe(III) oxide-rich sediment slurries were amended with different amounts of labile organic matter demonstrated a direct correlation between first-order Fe(III) reduction rate constants and initial rates of organic carbon mineralization. These results provide empirical support for existing approaches to modeling organic matter decay-dependent Fe(III) oxide reduction kinetics in sediments.

Fe(III) oxides together with aqueous and solid-phase Fe(II) compounds are abundant components of many hydromorphic soils and aquatic sediments, and the redox cycling of Fe exerts a wide-ranging influence on the biogeochemistry of sedimentary environments where Fe is abundant (Ponnamperuma 1972; Lovley 1991; Davison 1993). Recent studies in both freshwater (Roden and Wetzel 1996) and marine (Canfield et al. 1993; Thamdrup et al. 1994; Hines et al. 1997; Thamdrup 2000) habitats indicate that dissimilatory microbial Fe(III) oxide reduction contributes substantially to sediment carbon metabolism. Microbial Fe(III) oxide reduction can play a major role in suppressing methanogenesis in freshwater environments, both in surface sediments (Lovley and Phillips 1986b; Achnich et al. 1995; Roden and Wetzel 1996) and in the rhizosphere of aquatic plants (Roden and Wetzel 1996; Van Der Nat and Middelburg 1998; Frenzel et al. 1999) where oxygen input from plant roots drives a dynamic Fe redox cycle.

Although a large body of knowledge exists on sedimentary Fe transformations and their environmental significance (e.g., Lovley 1991; Stumm and Sulzberger 1992; Davison 1993), detailed information on the in situ kinetics of many

key processes is still not available. Understanding the kinetics of microbial Fe(III) oxide reduction is a prerequisite for modeling carbon and energy flux through sedimentary Fe cycling and the impact of Fe(III) oxide reduction on other electron-accepting processes (Thamdrup 2000), as well as for predicting the fate of inorganic and organic contaminants whose behavior is linked to Fe redox chemistry (Van Cappellen and Wang 1995). To date there has been no definitive demonstration of the kinetics of this process, e.g., in a manner analogous to how the kinetics of bacterial sulfate reduction in marine sediments has been defined in relation to sulfate and particulate organic carbon concentration (Boudreau and Westrich 1984; Westrich and Berner 1984). Analysis of the kinetics of microbial Fe(III) reduction in sediments presents a unique problem relative to other terminal electron-accepting reactions (e.g., oxygen, nitrate, and sulfate reduction) because Fe(III) oxides are highly insoluble at circumneutral pH. As a result, the reduction process involves the interaction of bacterial cell surfaces with particulate oxide phases that are not transported into the cell (Lovley 1987; Ghiorse 1988).

We report here on the kinetics of amorphous Fe(III) oxide (referred to hereafter simply as Fe(III) oxide) reduction in sediments of a freshwater wetland in north central Alabama, USA. The goal was to resolve basic quantitative features of microbial Fe(III) oxide reduction in a representative Fe-rich freshwater sediment. The wetland site provides an ideal venue for this analysis because sulfide-linked Fe(III) reduction is minor as a result of low sulfate abundance and sediment Fe diagenesis is therefore dominated by direct enzymatic Fe(III) reduction (Roden and Wetzel 1996).

Materials and methods

Study site—Sediments were obtained from a freshwater wetland located in the Talladega National Forest in north

¹ Corresponding author (eroden@bsc.as.ua.edu).

² Current address: Department of Environmental Sciences and Engineering, The University of North Carolina, Chapel Hill, North Carolina 27599-7431.

Acknowledgments

We thank Kim Warner for review of an earlier version of the manuscript. We also thank two anonymous reviewers and Associate Editor J.J. Middelburg for their constructive input to the paper. This work was supported by grant DEB-9407233 from the U.S. National Science Foundation, Ecosystem Studies Program; and grants DE-FG07-96ER62317 and DE-FG07-96ER62321 from the U.S. Department of Energy, Environmental Management Science Program. This paper is a contribution from the Center for Freshwater Studies, The University of Alabama.

central Alabama, USA. The wetland was formed ca. 50 yr ago by beaver activity that flooded 1.5 ha of forest floor. Talladega Wetland (TW) waters are soft (alkalinity = 0.05–0.1 meq L⁻¹, conductivity = 8–50 μ S cm⁻¹) and weakly acidic (pH 5.5–6.8) (Stanley and Ward 1997). Approximately 10–15 cm of organic-rich (20–30% dry weight) unconsolidated sediment has accumulated over the original forest soil since impoundment (Mann and Wetzel 2000). The sediments are rich in Fe (ca. 5% dry weight) owing to the Fe-rich Ultisol soil regime in which the wetland is situated. Overlying water nitrate concentrations are low (<1 μ M; Stanley and Ward 1997), and solid-phase Mn is 100-fold less abundant than Fe (E. Roden, unpubl. data). Hence nitrate and Mn(IV) oxide reduction are likely insignificant in sediment carbon metabolism in TW sediments. In addition, sulfate concentrations are in the low range for freshwater systems (<40 μ M), which strongly limits the role of sulfate reduction in sediment carbon metabolism and Fe diagenesis (Roden and Wetzel 1996). The majority (ca. 80%) of total reactive Fe in TW sediments (as determined by citrate-dithionite extraction; Canfield 1989) is in the form of 0.5 M HCl-extractable Fe, which comprises amorphous Fe(III) oxides and solid-phase Fe(II) compounds (Roden and Wetzel 1996; Roden and Edmonds 1997). Concentrations of amorphous Fe(III) oxide are high (20–75 mmol L⁻¹) in surface sediments and decrease rapidly with depth as a result of intensive bacterial reduction (Roden and Wetzel 1996).

Sediment sampling and Fe analysis—Undisturbed sediment cores were obtained manually with 10-cm ID Plexiglas tubes with a sharpened edge at the bottom. Sediment cores were returned to the laboratory and held at room temperature (22 \pm 1°C) overnight before being transferred to an anaerobic chamber (Coy Products) and sectioned at 0.25- to 1.0-cm intervals. On two occasions, surface sediment (0–0.25 cm) was collected with a 60-ml plastic syringe, and the sediments were quickly transferred to a 125-ml flask, which was completely filled and sealed with a rubber stopper. Subsequent manipulation of the surface sediments was carried out in the anaerobic chamber. Concentrations of amorphous Fe(III) oxide and total Fe(II) (solid + dissolved) were quantified by extracting (1 h) 0.1- to 0.5-ml volumes of sediment with 5–10 ml of 0.5 M HCl, followed by colorimetric (Ferrozine) determination of Fe(II) and total Fe in 0.025- to 0.1-ml aliquots of the extracts (Roden and Lovley 1993). Fe(III) was calculated from the difference between total Fe and Fe(II).

Surface sediment incubation experiments—Fe(III) oxide reduction was monitored in homogenized sediment from different depth intervals in the upper 3 cm of TW sediments, with material combined from three or four replicate cores. On two occasions, Fe(III) reduction was studied in homogenized surface sediment (0–0.25 cm) collected with a plastic syringe (see above). Portions of homogenized sediment (2–3 ml) were incubated (in the dark at room temperature) under N₂ in 15-ml serum vials over a 2–3 week period. Replicate vials were sacrificed at 1–5-d intervals (2 or 3 samples per time point) for measurements of 0.5 M HCl-extractable Fe(III) and Fe(II) concentration. Production of Σ CO₂ (gas-

eous CO₂ + dissolved inorganic carbon) and CH₄ was measured during these experiments with a previously described gas chromatographic approach (Roden and Wetzel 1996). Although methanogenesis was inhibited during the initial stages of Fe(III) oxide reduction, substantial production of CH₄ occurred toward the end of the incubations as Fe(III) was depleted. Therefore, it was necessary to estimate total rates of organic carbon mineralization in these and other experiments from the combined accumulation of Σ CO₂ and CH₄.

Sediment slurry experiments—Slurries were prepared with material from the upper 5–10 cm of sediment. Sediments were homogenized, passed through a 1-mm sieve, and mixed with anaerobic distilled water (1:1 v/v). The slurries were incubated in the dark at room temperature for ca. 2 weeks to deplete Fe(III) oxides. Portions of the slurry were then oxidized by stirring and bubbling with air for 24 h. This procedure converted virtually all (>90%) of the solid and dissolved Fe(II) in the sediment to amorphous, 0.5 M HCl-extractable Fe(III) oxide. The slightly acidic (pH 5–6) oxidized sediments were neutralized with NaOH and made anaerobic by sparging with O₂-free N₂:CO₂ (90:10%).

An inoculum (5% vol) of reduced sediment was added to oxidized slurries to reestablish anaerobic bacterial populations. Portions of sediment slurry (2–50 ml) were then transferred under N₂ to serum bottles (15–100 ml), and the bottles were sealed with thick rubber stoppers. In some experiments, replicate (2 or 3) larger bottles of sediment slurry (50 or 100 ml initial volume) were repeatedly sampled for 0.5 M HCl-extractable Fe(III) and Fe(II) at 1- to 5-d intervals over a 3- to 4-week incubation period. Samples (0.25 or 0.5 ml) were withdrawn from the bottles using N₂-flushed 1-ml syringes with 18 G disposable needles. In other experiments, replicate smaller bottles containing 2–3 ml of slurry were sacrificed at comparable intervals for determination of 0.5 M HCl-extractable Fe(III) and Fe(II). All sediment slurries were incubated in the dark at room temperature. Production of Σ CO₂ and CH₄ was measured via gas chromatography during one of the slurry experiments.

The rate of Fe(III) oxide reduction as a function of initial Fe(III) concentration was examined by combining different proportions of oxidized (Fe(III)-rich) and reduced (Fe(III)-depleted) sediment slurries and following the consumption of Fe(III) over time as described above.

The relationship between Fe(III) oxide reduction rate and labile organic matter (OM) abundance was investigated by following the consumption of Fe(III) over time in oxidized sediment slurries amended with different amounts of fresh OM (equivalent to 0, 0.125, 0.25, 0.5, 0.75, or 1.0% dry weight) in the form of heat-killed (80°C, 1 h) baker's yeast. Baker's yeast was used as a surrogate for phytoplankton-derived organic detritus in previous studies of the effect of OM on sediment metabolism (Caffrey et al. 1993). Production of Σ CO₂ and CH₄ was measured via gas chromatography in parallel with Fe(III) oxide reduction in this experiment. Once complete reduction of the Fe(III) oxide content of the different slurries was achieved (after 5 to 35 d, depending on the level of OM amendment), the abundance of dissimilatory Fe(III)-reducing bacteria (FeRB) was estimated

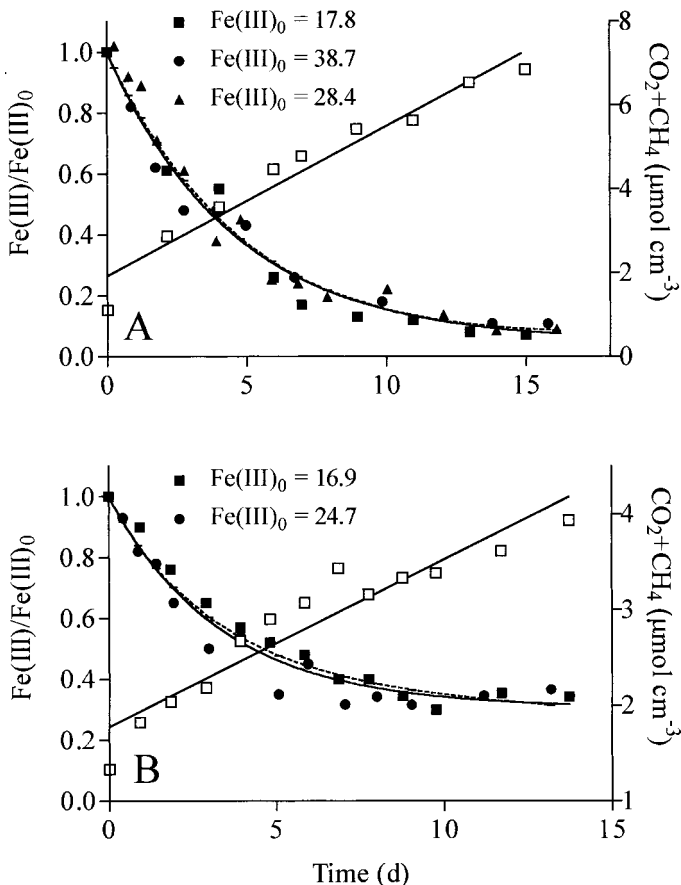


Fig. 1. Fe(III) reduction during anaerobic incubation of (A) oxidized TW sediment slurries and (B) TW surface sediments. The different symbols show averages of duplicate or triplicate bottles for separate experiments. Symbol legends indicate initial Fe(III) oxide concentrations in $\mu\text{mol cm}^{-3}$. Solid lines are nonlinear least-squares regression fits of pooled data to Eq. 1; dashed lines are nonlinear least-squares regression fits of the data to Eq. 14; best-fit parameter values are listed in Table 2. Open symbols show $\Sigma\text{CO}_2 + \text{CH}_4$ production during anaerobic incubation; the lines are linear least-squares regression fits.

with a most probable number (MPN) technique similar to that used previously for enumeration of FeRB in TW sediments (Coates et al. 1998). The bicarbonate-buffered (30 mM, pH 6.8) medium for MPN determinations contained (1) ca. $20 \mu\text{mol cm}^{-3}$ of synthetic amorphous Fe(III) oxide; (2) 10 mM acetate, 10 mM lactate, and 20% H_2 (in headspace); and (3) a mixture of vitamins and trace elements (Lovley and Phillips 1986b). The combination of acetate, lactate, and H_2 was assumed to provide suitable electron donors for all the major groups of dissimilatory Fe(III)-reducing bacteria (Lovley 2000). The culture medium was supplemented with 2 mM $\text{FeCl}_2 \cdot 2\text{H}_2\text{O}$ (added by needle and syringe from a filter-sterilized 200 mM stock solution) as a reductant prior to inoculation. Cultures were incubated in the dark at room temperature for 6 months. The presence of Fe(III) oxide reduction activity was assessed visually from color changes and was checked when necessary by 0.5 M HCl extraction and Fe(II) analysis. MPN estimates were obtained from tables 5–7 in Woormer (1994).

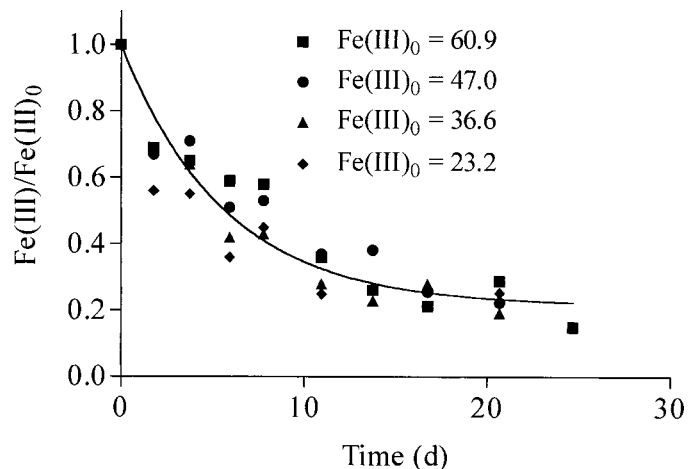


Fig. 2. Fe(III) reduction during anaerobic incubation of slurries containing different proportions of oxidized (Fe(III)-rich) and reduced (Fe(III)-depleted) TW sediment. Different symbols show averages of duplicate or triplicate bottles for four sets of slurries out of eight total. Symbol legends indicate initial Fe(III) oxide concentrations in $\mu\text{mol cm}^{-3}$. Solid lines are nonlinear least-squares regression fits of pooled data to Eq. 1; best-fit parameter values are listed in Table 2.

Abiotic Fe(III) oxide reduction by ascorbate—Rates of abiotic Fe(III) oxide reduction by ascorbate were determined for oxidized sediment slurries and surface (0–0.25 cm) sediments by the procedure described in Postma (1993). A small portion (0.5–1 ml) of slurry or surface sediment was added to 100 ml of O_2 -free 10 mM ascorbic acid (pH 3) to yield a final Fe(III) concentration of 0.4–0.5 $\mu\text{mol cm}^{-3}$. Concentrations of aqueous Fe(II) were monitored over time by filtering (0.45 μm) 1-ml subsamples into 5 ml of Ferrozine and immediately reading the A_{562} . Comparison of Fe(II) evolution during extraction of surface sediment with 10 mM ascorbate (pH 3) versus 1 mM HCl (pH 3) indicated that proton-promoted dissolution of endogenous Fe(II) phases (which in the case of TW surface sediment accounted for 20–30% of 0.5 M HCl-extractable Fe) did not influence the apparent kinetics of Fe(III) oxide reduction by ascorbate.

Results

Fe(III) oxide reduction time course experiments—Concentrations of amorphous Fe(III) oxide decreased exponentially over time to a nonzero asymptote during anaerobic incubation of oxidized TW sediment slurries (Fig. 1A) and homogenized TW surface sediments (Fig. 1B). The Fe(III) versus time data for these and other Fe(III) oxide reduction experiments were normalized to the initial Fe(III) oxide concentration (Fe(III)_0) in order to permit nonlinear regression analysis of pooled data from experiments with different starting Fe(III) concentrations (*see Discussion*). Similar patterns of Fe(III) oxide depletion were observed during anaerobic incubation of slurries containing different proportions of oxidized and reduced sediment (Fig. 2) and homogenized sediments from various depth intervals in the upper 3 cm of TW sediment cores (Fig. 3). In all of the experiments in

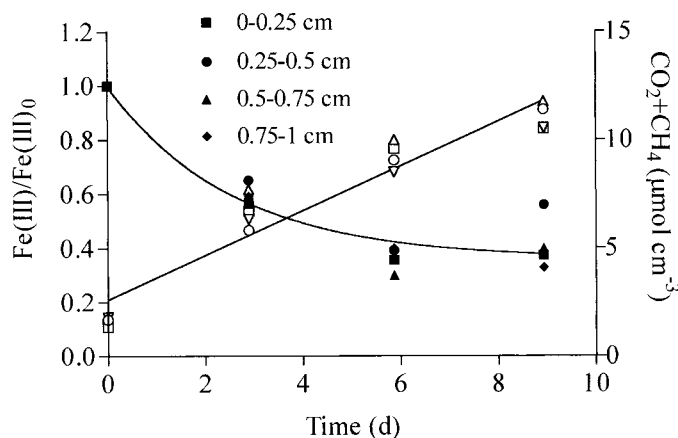


Fig. 3. Fe(III) reduction during anaerobic incubation of sediments from the 0–0.25, 0.25–0.5, 0.5–0.75 cm, and 0.75–1.0-cm depth intervals of TW sediment cores. Symbols represent averages of duplicate bottles sacrificed at each time point. Solid lines show nonlinear least-squares regression fits of the pooled data to Eq. 1; best-fit parameter values are listed in Table 2. Open symbols in each panel show $\Sigma\text{CO}_2 + \text{CH}_4$ production during anaerobic incubation; the line is a linear least-squares regression fit.

which rates of organic carbon mineralization were monitored, $\Sigma\text{CO}_2 + \text{CH}_4$ production was generally linear during the main period of Fe(III) reduction (Figs. 1 and 3; *see also Fig. 7B*). However, in some experiments (Figs. 1 and 7B), rates of $\Sigma\text{CO}_2 + \text{CH}_4$ evolution were somewhat higher during the first 5 d than during the following 1–2 weeks of incubation.

Initial Fe(III) oxide reduction rate versus Fe(III) oxide concentration—Initial Fe(III) oxide reduction rates in the mixtures of oxidized and reduced sediment (Fig. 2) were computed from the first derivative of nonlinear regression fits of Fe(III) versus time data to Eq. 1 below, evaluated at $t = 0$. The rates so obtained were linearly correlated with starting Fe(III) oxide concentration (Fig. 4, squares). A repeat of this experiment yielded comparable results (Fig. 4, circles). Initial rates of Fe(III) reduction in three separate core sectioning-incubation experiments were also linearly correlated with the starting Fe(III) oxide concentration (Fig. 5). Unlike rates of Fe(III) reduction, rates of total anaerobic carbon metabolism ($\Sigma\text{CO}_2 + \text{CH}_4$ production) were not strongly related to initial Fe(III) concentration in the upper few cm of TW sediment (Fig. 6A); only in the case of the third core sectioning-incubation experiment (Fig. 6A, triangles) was there a significant correlation between initial Fe(III) oxide abundance and carbon decomposition rate. The fraction of total anaerobic carbon flow mediated by Fe(III) reduction was, however, strongly related to initial Fe(III) oxide abundance (Fig. 6B), increasing in a generally linear fashion from 0.1–0.15 at Fe(III) concentrations $<25 \mu\text{mol cm}^{-3}$ to greater than 0.7 at Fe(III) concentrations $>75 \mu\text{mol cm}^{-3}$.

Organic matter addition experiment—Addition of increasing amounts of labile OM to slurries of Fe(III) oxide-rich TW sediment caused increased rates of Fe(III) depletion

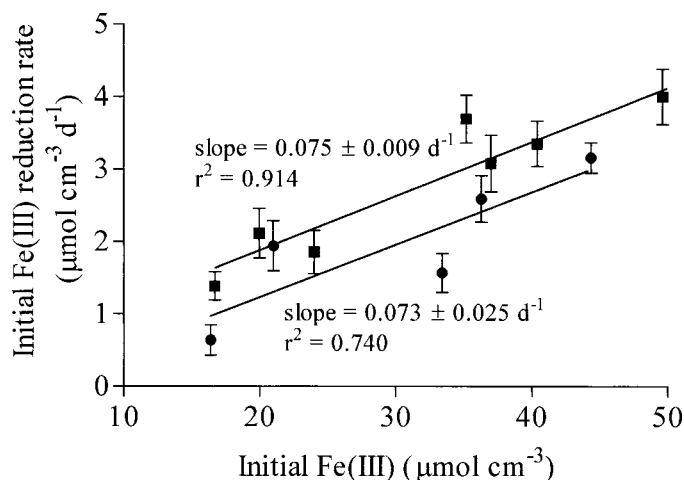


Fig. 4. Initial Fe(III) reduction rate versus initial Fe(III) oxide concentration in slurries containing different proportions of oxidized and reduced TW sediment. Initial rates were computed from the first derivative of nonlinear regression fits to Eq. 1, evaluated at $t = 0$. The different symbols show averages of triplicate bottles for two separate experiments. Error bars were computed from the standard error of the k_{red} and $[\text{Fe(III)}_0 - \text{Fe(III)}_{\text{nr}}]$ regression parameters via error propagation (Bevington and Robinson 1992). The line is a linear least-squares regression fit; the error term for the slope is the standard error of the regression parameter.

(Fig. 7A) and $\Sigma\text{CO}_2 + \text{CH}_4$ production (Fig. 7B). As in the slurry and surface sediment incubations, rates of $\Sigma\text{CO}_2 + \text{CH}_4$ production were essentially linear during the period of Fe(III) reduction (Fig. 7B, inset).

First-order Fe(III) reduction rate constants and initial rates of $\Sigma\text{CO}_2 + \text{CH}_4$ production increased linearly with increasing labile OM concentration and then approached an asymptote at the highest levels of OM addition (Fig. 8A). Rate constants and initial rates of Fe(III) oxide reduction were directly correlated with initial rates of $\Sigma\text{CO}_2 + \text{CH}_4$ evolution (Fig. 8B). The abundance of culturable FeRB estimated by MPN enumeration increased during anaerobic incubation from an initial density of ca. 1.4×10^6 cells ml⁻¹ to densities of 2.3×10^6 to 2.3×10^7 cells cm⁻³ in slurries amended with different amounts of OM (Table 1). FeRB abundance was not correlated with OM addition or Fe(III) reduction rate above 0.25% OM.

Discussion

Quantitative description of amorphous Fe(III) oxide reduction kinetics—A variety of studies have reported an exponential-like decrease in Fe(III) oxide concentration (or mirror image increase in Fe(II)) during anaerobic sediment incubation experiments (Lovley and Phillips 1986a; Jugsujinda et al. 1987; Lovley and Phillips 1987; Achtnich et al. 1995; Roden and Wetzel 1996; Frenzel et al. 1999; van Bodogom and Scholten 2001). Although these findings were suggestive of a first-order relationship between Fe(III) oxide concentration and reduction rate, the data were generally not interpreted in terms of a kinetic rate law, except in van Bodogom and Scholten (2001), in which a Monod kinetic ex-

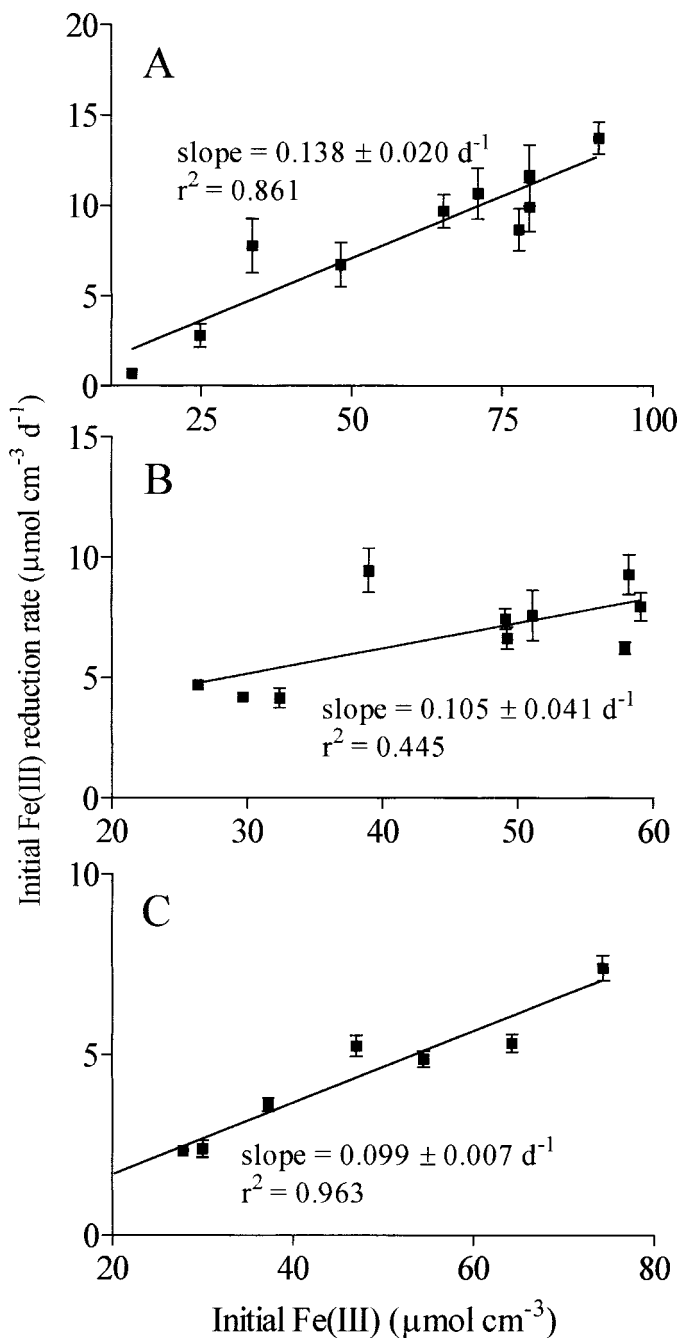


Fig. 5. Initial Fe(III) reduction rate versus initial Fe(III) concentration in sediments from different depth intervals in the upper 3 cm of TW sediment cores. Panels A, B, and C show results of experiments with cores collected on three different dates. Initial rates were computed from the first derivative of nonlinear regression fits to Eq. 1, evaluated at $t = 0$ (panel A), or from linear least-square regression analysis of Fe(III) versus time data (panels B and C). Error bars were computed from the standard error of the k_{red} and $[\text{Fe(III)}_0 - \text{Fe(III)}_{\text{nr}}]$ nonlinear regression parameters via error propagation (Bevington and Robinson 1992) (panel A), or from the standard error of the linear regression slope parameter (panels B and C). The line in each panel is a linear least-squares regression fit; the error term for the slope is the standard error of the regression parameter.

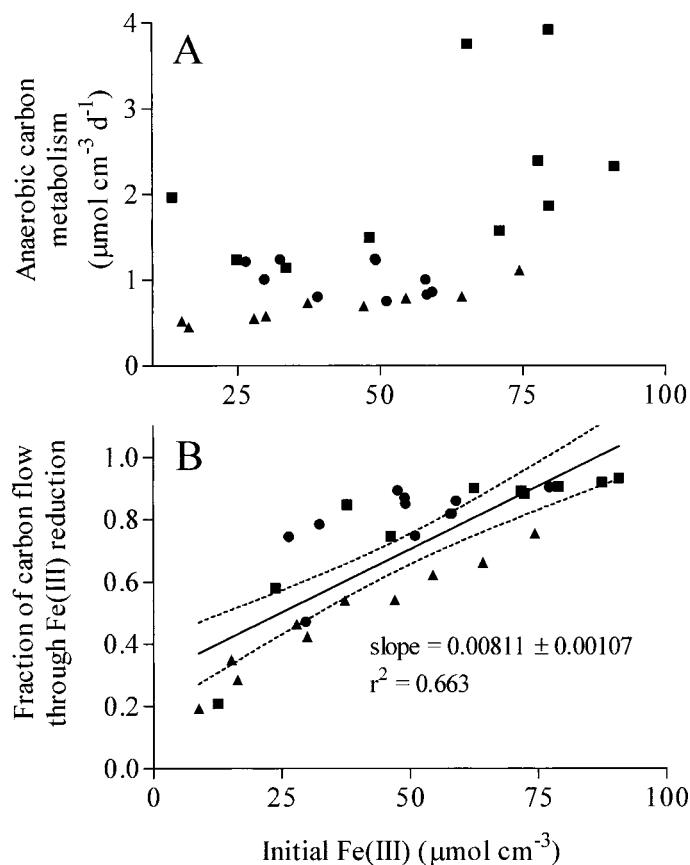


Fig. 6. (A) Rates of anaerobic carbon metabolism ($\Sigma\text{CO}_2 + \text{CH}_4$ production) and (B) fraction of total anaerobic carbon metabolism accounted for by Fe(III) reduction versus initial Fe(III) concentration in sediments from different depth intervals in the upper 3 cm of TW sediment cores. Different symbols show results of experiments with cores collected on three different dates. Solid line in panel B is a linear least-squares regression fit; dashed lines indicate the 95% confidence interval of the regression line; the error term for the slope is the standard error of the regression parameter.

pression was used to describe electron acceptor limitation of various anaerobic respiratory processes, including Fe(III) oxide reduction.

The Fe(III) reduction time course data in Figs. 1–3 were pooled and fitted by nonlinear least-squares regression analysis (GraphPad Prism® software) to the following equation:

$$\frac{\text{Fe(III)}_{(t)}}{\text{Fe(III)}_0} = \frac{[\text{Fe(III)}_0 - \text{Fe(III)}_{\text{nr}}]}{\text{Fe(III)}_0} \exp(-k_{\text{red}}t) + \frac{\text{Fe(III)}_{\text{nr}}}{\text{Fe(III)}_0} \quad (1)$$

where $\text{Fe(III)}_{(t)}$ is the Fe(III) oxide concentration at time t , Fe(III)_0 is the initial Fe(III) oxide concentration, $\text{Fe(III)}_{\text{nr}}$ is the nonreactive Fe(III) oxide concentration, and k_{red} is a first-order rate constant. Both k_{red} and the parameter group $\text{Fe(III)}_{\text{nr}}/\text{Fe(III)}_0$ were all allowed to vary during the fitting procedure. Best-fit regression parameters are listed in Table 2. Eq. 1 is an integrated form of the first-order rate expression

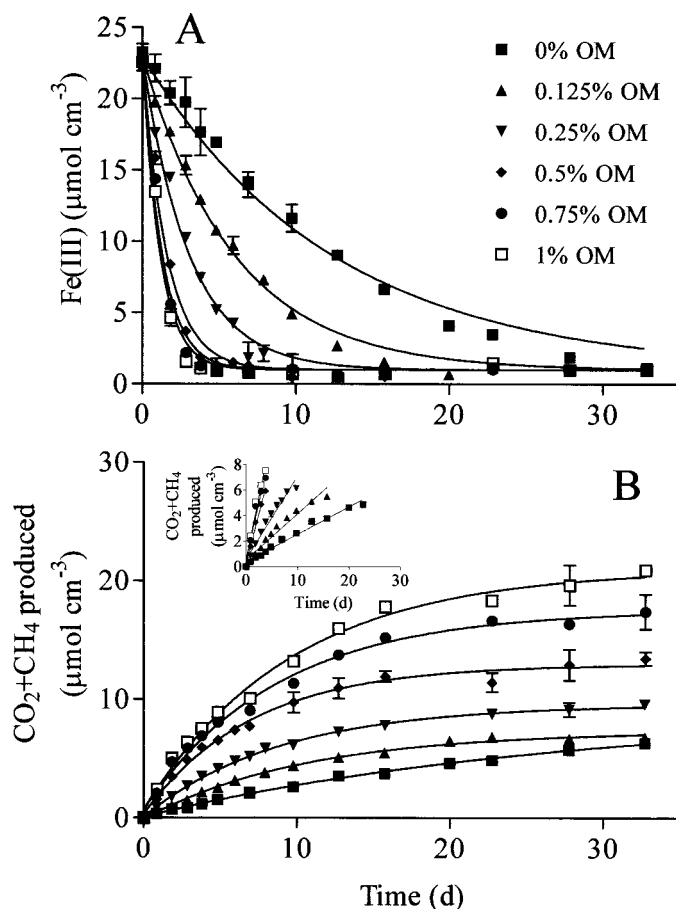


Fig. 7. (A) Fe(III) reduction and (B) organic carbon mineralization during anaerobic incubation of oxidized TW sediment slurries amended with different amounts (in percentage dry weight) of labile organic matter (OM). Each symbol shows the mean \pm range of duplicate bottles. Solid lines in panel A show nonlinear least-squares regression fits of the data to Eq. 1. Solid lines in panel B show nonlinear least-squares regression fits of the data to an equation of the form $C(t) = C_{\max}[1 - \exp(-at)]$, where $C(t)$ represents the amount of $\Sigma\text{CO}_2 + \text{CH}_4$ produced at time t , C_{\max} represents the maximum (asymptotic) amount of $\Sigma\text{CO}_2 + \text{CH}_4$ produced during the incubation period, and a represents a first-order rate constant. Inset in panel B shows initial rates of $\Sigma\text{CO}_2 + \text{CH}_4$ production; lines in are linear least-squares regression fits.

$$\begin{aligned} \frac{d\text{Fe(III)}_{(t)}}{dt} &= -k_{\text{red}}[\text{Fe(III)}_{(t)} - \text{Fe(III)}_{\text{nr}}] \\ &= -k_{\text{red}}\text{Fe(III)}_{\text{reac}} \end{aligned} \quad (2)$$

which is analogous to the equation used by Westrich and Berner (1984) for kinetic analysis of POC decomposition. Note that the quantity $(\text{Fe(III)} - \text{Fe(III)}_{\text{nr}})$ represents the reactive Fe(III) oxide content, abbreviated as $\text{Fe(III)}_{\text{reac}}$. The nonreactive (i.e., nonmicrobially reducible) Fe(III) oxide in TW sediments probably represents moderately crystalline Fe(III) oxides that were subject to dissolution by 0.5 M HCl but not readily susceptible to microbial reduction on the time scale of our experiments. The presence of such nonreducible, 0.5 M HCl-extractable Fe(III) in TW surface sediments is consistent with previous observations of the persistence of

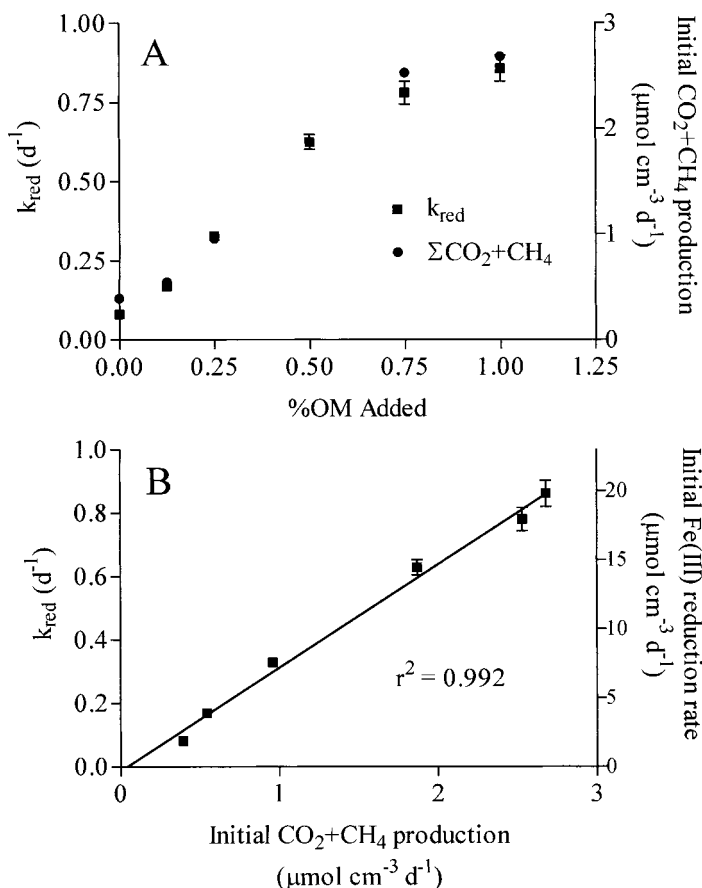


Fig. 8. (A) First-order Fe(III) reduction rate constants and initial $\Sigma\text{CO}_2 + \text{CH}_4$ production rates for oxidized TW sediments slurries amended with different amounts (in percentage dry weight) of labile organic matter (OM). Fe(III) reduction rate constants were obtained from nonlinear regression fits of the data in Fig. 7A to Eq. 1. Initial $\Sigma\text{CO}_2 + \text{CH}_4$ production rates were estimated from the first derivative of nonlinear regression fits of the data in Fig. 7B to the equation given in the Fig. 7 legend, evaluated at $t = 0$. (B) Fe(III) reduction rate constants and initial Fe(III) reduction rates versus initial $\Sigma\text{CO}_2 + \text{CH}_4$ production rates from panel A. Initial Fe(III) reduction rates were estimated from the first derivative of nonlinear regression fits in Fig. 7A, evaluated at $t = 0$. Line shows the result of a linear least-squares regression analysis.

Table 1. MPN estimates of FeRB abundance in sediments amended with different amounts (in percentage dry weight) of labile organic matter (OM). MPN enumerations were initiated in un-amended sediments at the start of the experiments (time zero), and at the end of the period of Fe(III) reduction (after 5–35 d) for each of the OM amendments.

Treatment	MPN estimate (cells cm^{-3})	95% confidence interval
Time zero	1.44×10^6	$3.09 \times 10^5 - 6.72 \times 10^6$
0% OM	2.30×10^6	$4.93 \times 10^5 - 1.07 \times 10^7$
0.125% OM	4.26×10^6	$9.12 \times 10^5 - 1.98 \times 10^7$
0.25% OM	2.31×10^7	$4.95 \times 10^6 - 1.08 \times 10^8$
0.5% OM	2.31×10^7	$4.95 \times 10^6 - 1.08 \times 10^8$
0.75% OM	2.31×10^7	$4.95 \times 10^6 - 1.08 \times 10^8$
1% OM	2.31×10^7	$4.95 \times 10^6 - 1.08 \times 10^8$

Table 2. Results of nonlinear least-squares regression analyses of pooled Fe(III) oxide reduction time course data according to Eqs. 1 and 14.

Experiment	Figure	Parameter	Best-fit value*	<i>n</i>	<i>r</i> ²
Slurries	1A	Fe(III) _{nr} /Fe(III) ₀	0.048±0.026	35	0.975
		<i>k</i> _{red}	0.220±0.016		
Slurries	1A	<i>a</i>	51.5±21.9	35	0.957
		<i>ν</i>	13.2±5.4		
		(1 + 1/ <i>ν</i>)	1.08		
		Fe(III) _{nr} /Fe(III) ₀	0.306±0.023		
Surface sediment	1B	<i>k</i> _{red}	0.296±0.029	27	0.959
		<i>a</i>	65.7±31.1		
Surface sediment	1B	<i>ν</i>	20.5±9.4	27	0.931
		(1 + 1/ <i>ν</i>)	1.05		
		Fe(III) _{nr} /Fe(III) ₀	0.214±0.031		
		<i>k</i> _{red}	0.178±0.021		
Mixed oxidized and reduced sediment	2	Fe(III) _{nr} /Fe(III) ₀	0.358±0.039	36	0.907
Core sectioning and incubation	3	<i>k</i> _{red}	0.392±0.080	32	0.893
		Fe(III) _{nr} /Fe(III) ₀	0.313±0.050		
Slurry ascorbate reduction	9A	<i>a</i>	0.977±0.094	20	0.991
		<i>ν</i>	2.02		
		(1 + 1/ <i>ν</i>)	1.43±0.25		
		Fe(III) _{nr} /Fe(III) ₀	0.313±0.050		
Surface sediment ascorbate reduction	9B	<i>a</i>	1.41±0.17	41	0.987
		<i>ν</i>	1.71		
		(1 + 1/ <i>ν</i>)	1.71		
		Fe(III) _{nr} /Fe(III) ₀	0.313±0.050		

* Error terms represent the standard error of the nonlinear regression parameter.

0.5 M HCl-extractable Fe(III) at depths below the zone of active Fe(III) oxide reduction in TW sediments (Roden and Wetzel 1996). Wallmann et al. (1993) also documented low but significant concentrations of 1 M HCl-extractable Fe(III) at depth in freshwater (riverine) sediments.

The close adherence of the Fe(III) oxide reduction time course data to Eq. 1 provides explicit evidence that rates of microbial amorphous Fe(III) oxide reduction in TW sediments are first order with respect to reactive Fe(III) oxide concentration. It is important to note, however, that because overall rates of organic carbon mineralization ($\Sigma\text{CO}_2 + \text{CH}_4$ production) decreased somewhat after the first 5 d of incubation (see Fig. 1), the curvilinear decline in Fe(III) oxide concentration over time may be attributed at least partly to a decline in OM decay rate as well as to the effect of Fe(III) limitation. Although the decline in OM decay rate does not invalidate the general conclusion of first-order kinetics for Fe(III) reduction, it does affect the value of rate constants derived from curve fitting of Fe(III) versus time data (see Eq. 10 and further discussion below). Hence, the *k*_{red} values reported in Table 2 must be considered pseudo first-order rate constants that include the effects of both OM and Fe(III) limitation.

Further support for a first-order relationship between Fe(III) oxide reduction rate and concentration comes from experiments that demonstrated that initial rates of Fe(III) oxide reduction were directly (linearly) correlated with starting Fe(III) oxide concentrations in sediment slurries (Fig. 4) and surface sediments (Fig. 5). In the experiments with mixtures of oxidized and reduced sediments (Fig. 4), equal amounts of reactive OM were present in all of the slurries so that the observed correlation between Fe(III) oxide concentration and reduction rate should not have been confounded by differences in labile OM decay rate (which were not quantified in these experiments). Similarly, rates of organic carbon

mineralization were relatively uniform in the upper few cm of TW sediment (Fig. 6A). These findings indicate that the direct correlation between initial Fe(III) reduction rate and Fe(III) oxide concentration illustrated in Figs. 4 and 5 can be robustly interpreted as a first-order response of Fe(III) reduction rate to Fe(III) oxide abundance in TW sediments.

Two recent studies in marine systems have demonstrated direct correlations between Fe(III) oxide reduction rate and amorphous Fe(III) oxide abundance: Hines et al. (1997) found that rates of Fe(III) reduction (monitored by dissolved Fe(II) accumulation) during slurry incubations of sediments from the northern Adriatic Sea were linearly correlated with initial concentrations of hydroxylamine HCl-extractable Fe(III); and Thamdrup (2000) reported that downcore Fe(III) reduction rates in Danish coastal sediments (estimated by the difference between ΣCO_2 production and sulfate reduction rates during anaerobic sediment incubations) closely paralleled the distribution of poorly crystalline Fe(III) oxide as determined by anaerobic oxalate extraction. It is important to note that some portion of the Fe(III) oxide reduction activity observed in the Adriatic Sea sediment incubations may have been linked to oxidation of sulfide produced during bacterial sulfate reduction, which was shown to occur at substantial rates within the zone of Fe(III) reduction in the upper 10 cm of sediment. Nevertheless, these studies collectively provide strong evidence for a first-order relationship between amorphous Fe(III) oxide reduction rate and concentration in aquatic sediments.

None of the Fe(III) reduction rate versus concentration data obtained in this study provided obvious indication of saturation of reduction rate with respect to Fe(III) concentration at high Fe(III) abundance. Although rates of Fe(III) reduction at the highest Fe(III) concentrations were often not statistically different from one another, the general trend of the rate versus concentration data (Figs. 4 and 5) was linear

rather than hyperbolic. Assuming that total rates of organic carbon mineralization were essentially equal across the range of Fe(III) concentrations present within a given batch of sediment (*see above*), a linear relationship between Fe(III) reduction rate and Fe(III) concentration implies that the fraction of total anaerobic carbon metabolism mediated by Fe(III) oxide reduction should also have been linearly related to Fe(III) concentration. Data from the three core sectioning/incubation experiments (Fig. 6B) support this assertion: despite substantial scatter in the data, a general linear trend is evident between the fraction of carbon flow through Fe(III) reduction and the initial Fe(III) concentration, with Fe(III) reduction accounting for ca. 90% of metabolism at Fe(III) concentrations approaching $100 \mu\text{mol cm}^{-3}$. Thamdrup (2000) reported an analogous relationship for marine sediments, in which percent carbon flow through Fe(III) reduction increased linearly to ca. 90% as poorly crystalline Fe(III) oxide concentrations increased from 0 to ca. $30 \mu\text{mol cm}^{-3}$. Rates of Fe(III) reduction and percent carbon flow through Fe(III) reduction would be expected to approach a maximum value at very high Fe(III) abundance, and in fact the data in Fig. 6B and in fig. 5 of Thamdrup (2000) give some indication of saturation of percent carbon flow through Fe(III) reduction at the highest Fe(III) concentrations. However, within the scatter of the data it is not possible to state definitively whether such saturation was operative. In general, available data suggest that Fe(III) reduction rates and percent carbon flow through Fe(III) reduction are linearly related to reactive Fe(III) abundance at the Fe(III) concentrations typically observed in aquatic sediments.

Theoretical basis for first-order rate model—The observed first-order kinetics of microbial Fe(III) oxide reduction can be rationalized in terms of established theories of chemical (abiotic) mineral transformation. Chemical dissolution of metal oxide and silicate minerals is commonly described by the following generalized rate law (Hering and Stumm 1990; Stumm and Sulzberger 1992):

$$R_{\text{surf}}(t) = -kC_{\text{surf}}(t) \quad (3)$$

where $R_{\text{surf}}(t)$ is the surface area-normalized dissolution rate (e.g., in $\mu\text{mol m}^{-2} \text{d}^{-1}$) at time t , k is a rate constant (d^{-1}), and $C_{\text{surf}}(t)$ is the concentration of surface species ($\mu\text{mol m}^{-2}$) involved in the dissolution reaction present at time t . Here surface species refers to an oxide surface coordinated with H^+ , OH^- , or organic ligands that polarize, weaken, and ultimately break the metal-oxygen bonds in the lattice of the oxide surface (Stumm and Sulzberger 1992). This formulation assumes that reactions at the Fe(III) oxide surface are surface controlled, i.e., that reactions at the surface are slow in comparison with other reaction steps, such as association of the ligand with the mineral surface to produce a surface species (Stumm and Morgan 1996). A well-known example of abiotic mineral dissolution is the reductive dissolution of crystalline hematite ($\alpha\text{-Fe}_2\text{O}_3$) by ascorbic acid (Sulzberger et al. 1989; Suter et al. 1991). The R_{surf} for this reaction is dependent on the concentration of ascorbate adsorbed to the oxide surface, which in turn is related to the concentration of ascorbic acid in solution according a Langmuir adsorption isotherm (Hering and Stumm 1990).

A conceptual analogy can be drawn between abiotic Fe(III) oxide reductive dissolution by surface-bound chemical reductants and enzymatic Fe(III) oxide reduction by dissimilatory FeRB, although the analogy is not a direct one because microbial Fe(III) oxide reduction produces solid-phase as well as dissolved Fe(II) species (for example, dissolved Fe(II) liberation accounted for only 5–10% of total Fe(II) production in the experiments shown in Figs. 1–4; *see* Roden and Wetzel 1996 and Roden and Edmonds 1997 for discussion of the importance of solid-phase Fe(II) end-products of microbial Fe(III) oxide reduction). Unlike soluble electron acceptors for microbial respiration, particulate Fe(III) oxides are not taken up into the cell (Lovley 1987). Rather, membrane-bound Fe(III) reductase systems transfer electrons to the oxide surface by mechanisms whose details are not yet fully understood (Lovley 2000). The immediate consequence of this fact is that microbial Fe(III) oxide reduction is a surface-controlled reaction between FeRB cells and particulate Fe(III) oxides. As such, surface area-specific rates of Fe(III) oxide reduction must be controlled by the abundance of active Fe(III) reductase systems in contact with oxide surface sites, i.e., the abundance of active reductase systems will determine the rate constant for surface area-specific enzymatic Fe(III) oxide reduction. The magnitude of this rate constant will be a complex function of the rate at which electron donors for Fe(III) oxide reduction are liberated through particulate OM hydrolysis and fermentation, the abundance of FeRB cells, and the relative susceptibility of oxide surface sites to reduction. The abundance of FeRB, in turn, will be dynamically controlled by the rate of electron donor supply, the abundance of reducible Fe(III) oxide surface sites, and the growth and death rates of the FeRB cells.

It is relevant to note here that effective rate constants for Fe(III) oxide reduction as well as rates of FeRB growth may be affected significantly by the presence of Fe(III) chelators and/or soluble electron shuttling compounds (e.g., humic substances), both of which are known to accelerate enzymatic reduction of amorphous Fe(III) oxides (Lovley et al. 1996, 1998; Lovley and Woodward 1996). Recent studies suggest that such compounds are likely to be ubiquitous in natural sedimentary environments (Lovley 2000; Nevin and Lovley in press). Detailed modeling of Fe(III) oxide reduction kinetics in the presence of such compounds would require information on the mechanism of their reaction with Fe(III) oxide surfaces, as well as their concentration and turnover rate—neither of which are available for TW or any other aquatic sediment. However, because such reactions are likely to be surface-controlled processes analogous to the well-studied interactions of synthetic chelators and soluble reductants with Fe(III) oxide minerals (Stumm 1992; Stumm and Morgan 1996), as a first approximation the effect of chelators and/or electron shuttling compounds can be assumed to be incorporated into the effective rate constant for Fe(III) oxide reduction, thereby permitting interpretation of Fe(III) oxide reduction kinetics in terms of the simple kinetic framework developed below. In support of this assertion, recent studies in our laboratory showed that the presence of electron shuttling humic compounds did not alter the basic first-order nature of enzymatic Fe(III) oxide by an acetate-

oxidizing, Fe(III)-reducing enrichment culture obtained from TW surface sediments (Roden and Wetzel, unpubl. data).

Given some specified rate constant for electron transfer to particulate Fe(III) oxide surfaces, the relationship between surface area-specific and bulk volumetric mineral transformation rate can be defined as follows:

$$R_{\text{bulk}}(t) = R_{\text{surf}}(t)\psi_s(t)SA = -kC_{\text{surf}}(t)\psi_s(t)SA(t) \quad (4)$$

where $R_{\text{bulk}}(t)$ is the bulk volumetric reaction rate ($\mu\text{mol cm}^{-3} \text{d}^{-1}$) at time t , $\psi_s(t)$ is the concentration of solids per unit volume (g cm^{-3}) at time t , and $SA(t)$ is the specific surface area of the mineral ($\text{m}^2 \text{g}^{-1}$) at time t . The bulk molar concentration of mineral is defined by

$$C_{\text{bulk}}(t) = \psi_s(t)/\text{MW} \quad (5)$$

where MW is the molecular weight of the mineral ($\text{g } \mu\text{mol}^{-1}$). Substituting this expression into Eq. 4 yields the following equation for volumetric mineral reaction rate:

$$R_{\text{bulk}}(t) = dC_{\text{bulk}}(t)/dt = -kC_{\text{surf}}(t)SA(t)\text{MW}C_{\text{bulk}}(t) \quad (6)$$

The term $kC_{\text{surf}}(t)SA(t)\text{MW}$ in Eq. 6 can be identified as an effective rate constant, $k'(t)$:

$$k'(t) = kC_{\text{surf}}(t)SA(t)\text{MW} \quad (7)$$

If we assume that $C_{\text{surf}}(t)$ and $SA(t)$ remain constant over time, i.e., that reactive surface sites are efficiently regenerated and that mineral morphology and surface site density remain constant during reaction, Eq. 6 reduces to a simple first-order rate expression:

$$R_{\text{bulk}} = dC_{\text{bulk}}/dt = -k'C_{\text{bulk}} \quad (8)$$

which is easily integrated to yield an exponential decay equation:

$$C_{\text{bulk}}(t) = C_{\text{bulk}}^0 \exp(-k't) \quad (9)$$

where C_{bulk}^0 is the molar concentration of mineral present at $t = 0$. Note that Eq. 8 is identical to the simple first-order rate law for microbial Fe(III) oxide reduction depicted by Eq. 2.

The significance of Eqs. 4–9 is that they show that bulk-phase concentrations of an oxide mineral can decrease exponentially over time as a result of abiotic or enzymatic reduction, while surface-controlled reactions at the mineral-water interface are in steady state with respect to surface area-specific reaction rate. This concept has direct relevance to the microbial Fe(III) oxide reduction experiments conducted in this study. Because rates of electron donor supply through organic carbon mineralization, as indicated by $\Sigma\text{CO}_2 + \text{CH}_4$ production, were essentially constant during Fe(III) oxide reduction, effective rate constants for surface area-specific enzymatic reduction were approximately constant over time. Hence, a direct analogy can be drawn between the exponential decline in bulk Fe(III) oxide concentration observed in the microbial reduction experiments (Figs. 1–3 and 7A) and the evolution of bulk-phase mineral concentration predicted by Eq. 9.

The assumption of a time-invariant effective rate constant for surface area-specific Fe(III) oxide reduction ignores the potential influence that changes in FeRB population size—and parallel changes in the abundance of active Fe(III) re-

ductase systems—could have on rates of bacterial mineral transformation. Strictly speaking, the use of such simplifications is not appropriate in quantitative models of micro-biologically catalyzed reactions in environmental systems (Rittman and Van Briesen 1996). However, this simplifying assumption is common (and often defensible) in geochemical models of sediment microbial processes (Boudreau 1992) and is used here in order to facilitate mechanistic interpretation of the overall kinetic response of microbial Fe(III) oxide reduction in TW sediments. As discussed further below, our knowledge of FeRB abundance is insufficient to permit accurate assessment of the importance of population size changes on apparent rate constants for microbial Fe(III) oxide reduction.

Influence of labile OM abundance on Fe(III) reduction kinetics—As emphasized in a recent review of bacterial Fe(III) oxide reduction in aquatic sediments (Thamdrup 2000), the abundance and decomposition rate of labile OM is expected to exert a major influence on the kinetics of Fe(III) oxide reduction in sediments. In order to explicitly evaluate the relationship between labile OM and Fe(III) oxide reduction kinetics, different amounts of labile OM were added to Fe(III) oxide-rich TW sediment slurries, and rates of OM mineralization and Fe(III) consumption were monitored. The results demonstrated direct correlations between the Fe(III) reduction rate constant, as well as the initial Fe(III) reduction rate, and the abundance (Fig. 8A) and mineralization rate (Fig. 8B) of labile OM. These findings are analogous to the demonstration by Westrich and Berner (1984) of a linear correlation between sulfate reduction rate and reactive organic carbon concentration in marine sediments. Since the y-intercept for the regression line in Fig. 8B is very close to zero, the reduction rate constant (k_{red}) and initial rate of Fe(III) oxide reduction (R_{init}) scale directly with OM decomposition rate ($R_{\text{CH}_2\text{O}}$) according to the simple relations

$$k_{\text{red}} = b_1 R_{\text{CH}_2\text{O}} \quad (10)$$

$$R_{\text{init}} = b_2 R_{\text{CH}_2\text{O}} \quad (11)$$

where b_1 and b_2 represent the slope of the line in Fig. 7B with either k_{red} or initial rate of Fe(III) reduction as the dependent variable.

It is possible to interpret the results of the OM addition experiment in relation to the surface area-controlled kinetic framework for microbial Fe(III) oxide reduction discussed above. The correlation between k_{red} and organic carbon mineralization can be attributed to a progressive increase in the rate constant for surface area-specific Fe(III) oxide reduction (k in Eq. 3) with increasing rates of electron donor liberation. These surface area-specific rate constants translate into increased effective rate constants for bulk Fe(III) depletion according to Eq. 7, which are equivalent to the k_{red} parameters obtained from curve fits of the Fe(III) time course data.

Based on the above findings, the following simple expression can be used to depict the combined influence of OM decay rate and reactive Fe(III) oxide abundance on Fe(III) oxide reduction rate:

$$R_{\text{Fe(III)}} = abR_{\text{CH}_2\text{O}}\text{Fe(III)}_{\text{reac}} \quad (12)$$

where α is the stoichiometric ratio between Fe(III) reduction and organic carbon oxidation (shown by Roden and Wetzel 1996 to closely approximate the theoretical value of 4.0) and the term $bR_{\text{CH}_2\text{O}}$ is equivalent to the effective k_{red} . This expression is functionally identical to the framework used in recent diagenetic models of Fe(III) oxide reduction and other biogeochemical processes in aquatic sediments (Boudreau 1996; Van Cappellen and Wang 1996). In this framework, Fe(III) oxide reduction rates are assumed to first order with respect to Fe(III) oxide abundance when the reactive Fe(III) concentration is below some prescribed "limiting" Fe(III) concentration (designated as $\text{Fe(III)}_{\text{lim}}$), and independent of Fe(III) oxide abundance when $\text{Fe(III)}_{\text{react}}$ is higher than $\text{Fe(III)}_{\text{lim}}$:

$$R_{\text{Fe(III)}} = \alpha R_{\text{CH}_2\text{O}} \text{Fe(III)}_{\text{react}} / \text{Fe(III)}_{\text{lim}} \quad \text{with } \text{Fe(III)}_{\text{react}} < \text{Fe(III)}_{\text{lim}} \quad (13a)$$

$$R_{\text{Fe(III)}} = \alpha R_{\text{CH}_2\text{O}} \quad \text{with } \text{Fe(III)}_{\text{react}} \geq \text{Fe(III)}_{\text{lim}} \quad (13b)$$

Equation 13 represents a linearized version of a hyperbolic (Monod-style) rate expression used to simplify the computation of Fe(III) oxide reduction rates in non-steady-state transport-reaction models. Comparison of Eqs. 12 and 13a shows the equivalence of b and the inverse of $\text{Fe(III)}_{\text{lim}}$. To our knowledge, the close adherence of our experimental data to Eq. 12 provides the first explicit empirical support for use of Eq. 13a for modeling OM-dependent Fe(III) oxide reduction kinetics in aquatic sediments. In addition, the lack of saturation of Fe(III) reduction rate with respect to Fe(III) oxide concentration documented in this and other studies (*see above*) suggests that use of Eq. 13b is in general not required for modeling Fe(III) oxide reduction kinetics in aquatic sediments, i.e., values of $\text{Fe(III)}_{\text{lim}}$ should be set high enough so that saturation of Fe(III) reduction rate does not occur within the range of reactive Fe(III) concentrations typically found in aquatic sediments.

Relationship between FeRB abundance and Fe(III) reduction kinetics—A MPN enumeration procedure employing synthetic growth medium was used to evaluate the potential importance of changes in FeRB population size to the response of microbial Fe(III) oxide reduction to addition of different amounts of labile OM. The results indicated that although FeRB abundance increased in OM-amended sediments compared to unamended slurries (Table 2), there was no correlation between FeRB abundance and OM addition above 0.25% OM. In contrast, rate constants for Fe(III) oxide reduction increased substantially in slurries amended with 0.25% to 1% OM (Fig. 7A). It is well known that MPN procedures employing synthetic growth media typically underestimate the abundance of anaerobic respiratory microorganisms such as sulfate-reducing bacteria by one or more orders of magnitude in both marine (Jorgensen 1978; Gibson et al. 1987; Ramsing et al. 1996; Vester and Ingvorsen 1998) and freshwater (Bak and Pfenning 1991) environments. The possibility thus exists that our MPN estimates did not accurately reflect the response of the sediment FeRB community to the addition of labile OM. Although the MPN results leave little doubt that addition of OM stimulated

FeRB growth, the true magnitude of this stimulation relative to the observed stimulation of Fe(III) oxide reduction cannot be determined. As a result, it is not possible to accurately assess the impact of changes in FeRB abundance on the kinetics of Fe(III) oxide reduction in the OM addition experiment. Refinement of MPN procedures for enumeration of FeRB (e.g., through use of natural media; Vester and Ingvorsen 1998) and/or application of molecular genetic techniques for non-culture-based estimation of FeRB abundance (e.g., MPN-PCR (polymerase chain reaction); Anderson et al. 1998; Rooney-Varga et al. 1999; Snoeyenbos-West et al. 2000) will be required in order to link variations in FeRB biomass to the bulk kinetics of Fe(III) oxide reduction in aquatic sediments.

Heterogeneity of Fe(III) oxide reactivity—Standard formulations for chemical oxide mineral dissolution assume that a single mineral of uniform specific surface area, reactive site density, and mineralogical stability is undergoing dissolution (Stumm 1992). In contrast, Fe(III) oxide assemblages in soils and sediments often possess a wide range of reactivity, owing to differences in mineralogy, crystallinity, grain size, and surface area (Postma 1993; Cornell and Schwertmann 1996). An important unresolved question is the extent to which heterogeneity in Fe(III) oxide reactivity influences the kinetics of bacterial Fe(III) oxide reduction in sediments (Postma 1993). In order to evaluate this question in relation to Fe(III) oxide reduction in TW sediments, data from sediment slurry and surface sediment incubation experiments (Figs. 1 and 3) were pooled and analyzed according to the reactive continuum model of Aris (1989) as described by Boudreau and Ruddick (1991) and Postma (1993). The concentration of Fe(III) designated as being formally nonreactive on the time scale of the incubation experiments was subtracted from measured Fe(III) values prior to conducting the reactive continuum analysis. For both the biotic and abiotic (ascorbate) Fe(III) reduction experiments, the nonreactive Fe(III) concentration was set equal to lowest Fe(III) concentration observed at the end of the incubation experiments.

The heterogeneity analysis involved fitting reactive Fe(III) versus time data to the following equation (Postma 1993):

$$m(t)/m_0 = [a/(a + t)]^\nu \quad (14)$$

where $m(t)$ is the mass (concentration) of reactive Fe(III) at time t , m_0 is the initial mass (concentration) of reactive Fe(III), and a and ν are curve-fit parameters. Rearrangement of this equation yields the following expression for the instantaneous rate of $\text{Fe(III)}_{\text{react}}$ reduction, $J(t)$, normalized to initial concentration of reactive Fe(III):

$$J(t)/m_0 = \nu/a[m(t)/m_0]^{1+1/\nu} \quad (15)$$

The exponent $(1 + 1/\nu)$ in this expression provides an indication of the degree of heterogeneity in reactivity of the oxides undergoing reduction, whereas the term ν/a represents an apparent rate constant for a mixture (Postma 1993). Values for $(1 + 1/\nu)$ of ca. 1.0 are expected for reductive dissolution of synthetic amorphous Fe(III) oxide (ferrihydrite) with uniform reactivity (Postma 1993). Higher values for this parameter grouping indicate the presence of a di-

versity of Fe(III) oxides with different intrinsic reactivities. As demonstrated by Postma (1993), Eq. 15 is functionally identical to the following general rate expression for dissolution of polydisperse crystals of a single mineral (Christoffersen and Christoffersen 1976):

$$J(t)/m_0 = k'[m(t)/m_0]^\gamma \quad (16)$$

where k' is a rate constant and γ is a parameter whose value is determined by the geometry and reactivity of the mineral crystals undergoing dissolution. As a result of the direct analogy between Eqs. 15 and 16, it is possible to obtain estimates of the terms (ν/a) and $(1 + 1/\nu)$ in Eq. 15 from nonlinear curve fits of Fe(III) reduction time course data to the integrated form of Eq. 16 (Larsen and Postma 2001):

$$m(t)/m_0 = [-k'(1 - \gamma)t + 1]^{1/(1-\gamma)} \quad (17)$$

Best-fit values for k' and γ obtained from fitting Fe(III) versus time data to Eq. 17 are synonymous with the terms (ν/a) and $(1 + 1/\nu)$ in Eq. 15. This strategy was preferable to fitting Fe(III) versus time data directly to Eq. 14, since the nonlinear curve-fitting procedure was generally more reliable (less prone to nonconvergence) when fitting such data to Eq. 17 compared to Eq. 14. In order to further improve the reliability of parameter estimates, an advanced nonlinear least-squares parameter estimation procedure that includes a model trust region (IMSL 1997) was employed. Testing showed that alteration of initial guess values for k' and γ in Eq. 17 by up to an order of magnitude did not alter the best-fit parameter estimates produced by the nonlinear fitting algorithm. Very large changes in initial guesses invariably produced negative values for either k' or γ , which have no mechanistic meaning. In all cases where nonnegative values were obtained for both k' and γ , the algorithm converged the same best-fit values.

Analysis of the microbial Fe(III) oxide reduction data in Fig. 1 (dashed lines) yielded values of 1.08 and 1.05 for the $(1 + 1/\nu)$ parameter group (Table 2). Analysis of data for abiotic Fe(III) oxide reduction by ascorbate according to the reactive continuum model (Fig. 9) yielded higher values for the $(1 + 1/\nu)$ parameter group than those obtained for the microbial reduction experiments (Table 2). It is important to note that the starting concentrations of Fe(III) oxide used to interpret the ascorbate reduction data were based on the same 0.5 M HCl extraction procedure used for the microbial Fe(III) reduction experiments. Thus, for the purposes of this analysis, the chemical and enzymatic reduction processes were acting as an equivalent pool of reactive Fe(III) oxide.

The results of the ascorbate reduction experiments indicated that amorphous Fe(III) oxides in TW sediments possess appreciable heterogeneity with respect to abiotic reductive dissolution. Although the values obtained for the $(1 + 1/\nu)$ parameter grouping (ca. 2) are smaller than those observed by Postma (1993) in similar experiments with oxidized marine sediments and shallow aquifer sediments (4.7 and 2.75, respectively), they nevertheless indicate that the rate of abiotic $\text{Fe(III)}_{\text{react}}$ reduction normalized to the initial $\text{Fe(III)}_{\text{react}}$ concentration (Eq. 15) decreased by a factor of ca. 4 after only a twofold decrease in total $\text{Fe(III)}_{\text{react}}$, and by a factor of ca. 100 after a tenfold decrease in $\text{Fe(III)}_{\text{react}}$. In comparison, the normalized dissolution rate for Fe(III) oxide

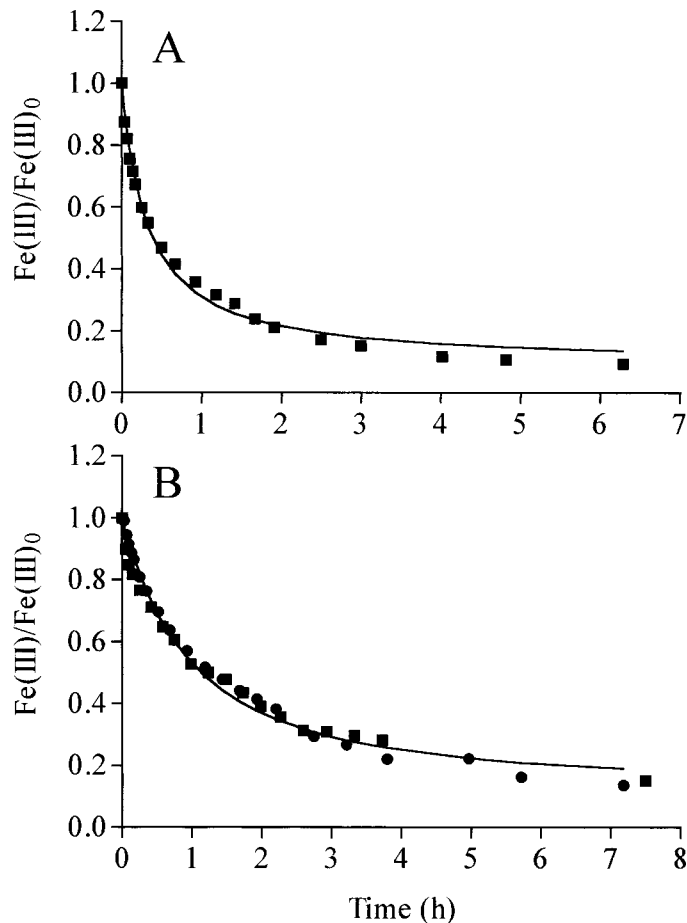


Fig. 9. Abiotic reduction of amorphous Fe(III) oxides in (A) TW sediment slurries and (B) mixed surface sediments by ascorbate (10 mM, pH 3), analyzed according to the reactive continuum model. Symbols in panel A show the results of a single experiment; symbols in panel B show results of two separate experiments. Solid lines are nonlinear least-squares regression fits of pooled data to Eq. 14; best-fit parameter values are listed in Table 2.

phases with uniform reactivity would be expected to decline in direct proportion to the concentration of $\text{Fe(III)}_{\text{react}}$ remaining.

In contrast to the results of the abiotic Fe(III) oxide reduction experiments, reactive continuum analysis of the microbial Fe(III) reduction data suggested that amorphous Fe(III) oxides in TW sediments were of relatively uniform reactivity with respect to enzymatic reduction (values for the $1 + 1/\nu$ parameter equal to ca. 1). The detailed time course data for microbial Fe(III) oxide reduction (Figs. 1–3), robustly described by a simple exponential decay equation, support this assertion, since by definition the slope of such an equation is linearly related to the value of the function at all points along the curve. The reason(s) for the apparent difference in heterogeneity of natural amorphous Fe(III) oxide reactivity with respect to chemical versus biological reduction is unclear. One possibility is that a larger fraction of the 0.5 M HCl-extractable Fe(III) content of TW sediments was susceptible to chemical reduction compared to microbial reduction, so that a more diverse spectrum of Fe(III) oxides

was included in the reactive continuum analysis of the abiotic reduction data. This argument is supported by the surface sediment reduction experiments in which a substantially greater fraction of the 0.5 M HCl-extractable Fe(III) content was reduced by ascorbate (ca. 90%) compared to microbial activity (ca. 75%). However, this was not the case for the oxidized slurry experiments, in which both ascorbate and microbial activity reduced ca. 90% of 0.5 M HCl-extractable Fe(III). Another possible explanation for the apparent difference in Fe(III) oxide heterogeneity with respect to biotic versus abiotic reduction is simply that enzymatic electron transfer responds less intensively than abiotic electron transfer to variations in Fe(III) oxide reactivity. Further consideration of this phenomenon is beyond the scope of the present work. The important point is that the uniformity of microbially reducible Fe(III) oxide phases with respect to enzymatic reduction suggests that the density of reaction sites per unit oxide surface area and their relative susceptibility to enzymatic reduction did not change appreciably during the reduction process. Hence, measured bulk Fe(III) concentrations should directly reflect the abundance of oxide surface sites that were available for microbial reduction, and correlations between Fe(III) reduction rate and bulk Fe(III) concentration (Figs. 4 and 5) reflect the dependence of reduction rate on bulk reactive Fe(III) oxide surface site abundance. These arguments fulfill fundamental criteria required for interpreting microbial Fe(III) oxide reduction as a surface-controlled process analogous to mineral transformation according to the framework depicted by Eqs. 4–9.

Relevance to reduction of crystalline Fe(III) oxides—Studies of microbial reduction of synthetic crystalline Fe(III) oxide have demonstrated a first-order relationship between initial rates of Fe(III) reduction and Fe(III) oxide concentration (Arnold et al. 1988; Roden and Zachara 1996; Roden and Urrutia 1999), as well as a direct correlation between the initial rate of reduction and the specific surface area of different crystalline Fe(III) oxide minerals (Roden and Zachara 1996). In terms of initial rates of activity, these results are in complete agreement with the data and theoretical interpretations for microbial reduction of natural amorphous Fe(III) oxides in TW sediments presented here. However, in contrast to natural amorphous Fe(III) oxides, the long-term extent of crystalline Fe(III) oxide reduction in batch culture experiments rarely exceeds 20% of the total Fe(III) content of the mineral(s) and is often limited to only a few percent (Lovley 1987; Roden and Zachara 1996; Zachara et al. 1998). Recent experimental studies suggest that the long-term extent of crystalline Fe(III) oxide reduction is controlled by the association of Fe(II) with oxide and FeRB cell surfaces, which inhibits enzymatic electron transfer to Fe(III) oxide surface sites (Urrutia et al. 1998; Roden and Urrutia 1999; Urrutia et al. 1999; Roden et al. 2000). These findings indicate that quantitative depiction of the kinetics of crystalline Fe(III) oxide reduction in sedimentary environments must account in some manner for the influence of Fe(II) surface complexation on the long-term degree of oxide reduction (Roden and Urrutia 1999). Conversely, studies to date suggest that amorphous Fe(III) oxides are subject to near-complete reduction in aquatic sediments, and as yet

there is no compelling suggestion that the influence of Fe(II) surface complexation needs to be accounted for in kinetic modeling of amorphous Fe(III) oxide reduction in these environments. Although the availability of surface sites on amorphous Fe(III) oxide particles undoubtedly controls the bulk rate of oxide reduction, the issue of whether amorphous Fe(III) oxide surface sites are occupied by adsorbed (or surface-precipitated) Fe(II) does not appear to be a crucial consideration with regard to bulk reduction kinetics. Hence, simulation of Fe(III) oxide reduction in sediments where amorphous Fe(III) oxide is the dominant form of Fe(III) available for microbial reduction can be appropriately conducted with the simple OM decay-dependent first-order rate model discussed in this paper.

References

- ACHTNICH, C., F. BAK, AND R. CONRAD. 1995. Competition for electron donors among nitrate reducers, ferric iron reducers, sulfate reducers, and methanogens in anoxic paddy soil. *Biol. Fert. Soils* **19**: 65–72.
- ANDERSON, R. T., J. N. ROONEY-VARGA, C. V. GAW, AND D. R. LOVLEY. 1998. Anaerobic benzene oxidation in the Fe(III) reduction zone of petroleum-contaminated aquifers. *Environ. Sci. Technol.* **32**: 1222–1229.
- ARIS, R. 1989. Reactions in continuous mixtures. *Am. Inst. Chem. Eng. J.* **35**: 539–548.
- ARNOLD, R. G., T. J. DICHRISTINA, AND M. R. HOFFMAN. 1988. Reductive dissolution of Fe(III) oxides by *Pseudomonas* sp. 200. *Biotechnol. Bioeng.* **32**: 1081–1096.
- BAK, F., AND N. PFENNING. 1991. Sulfate-reducing bacteria in littoral sediment of Lake Konstanz. *FEMS Microbiol. Ecol.* **85**: 43–52.
- BEVINGTON, P. R., AND D. K. ROBINSON. 1992. Data reduction and error analysis for the physical sciences. McGraw Hill.
- BOUDREAU, B. P. 1992. A kinetic model for microbial organic-matter decomposition in marine sediments. *FEMS Microbiol. Ecol.* **102**: 1–14.
- . 1996. A numerical-method-of-lines code for carbon and nutrient diagenesis in aquatic sediments. *Comput. Geosci.* **22**: 479–496.
- , AND B. R. RUDDICK. 1991. On a reactive continuum representation of organic matter diagenesis. *Am. J. Sci.* **291**: 507–538.
- , AND J. T. WESTRICH. 1984. The dependence of bacterial sulfate reduction on sulfate concentration in marine sediments. *Geochim. Cosmochim. Acta* **48**: 2503–2516.
- CAFFREY, J. M., N. P. SLOTH, H. F. KASPAR, AND T. H. BLACKBURN. 1993. Effect of organic loading on nitrification and denitrification in a marine sediment microcosm. *FEMS Microbiol. Ecol.* **12**: 159–167.
- CANFIELD, D. E. 1989. Reactive iron in marine sediments. *Geochim. Cosmochim. Acta* **53**: 619–632.
- , B. THAMDRUP, AND J. W. HANSEN. 1993. The anaerobic degradation of organic matter in Danish coastal sediments: Iron reduction, manganese reduction, and sulfate reduction. *Geochim. Cosmochim. Acta* **57**: 3867–3883.
- CHRISTOFFERSEN, J., AND M. R. CHRISTOFFERSEN. 1976. The kinetics of dissolution of calcium sulphate dihydrate in water. *J. Crystal Growth* **35**: 79–88.
- COATES, J. D., D. J. ELLIS, B. L. BLUNT-HARRIS, C. GAW, E. E. RODEN, AND D. R. LOVLEY. 1998. Recovery of humic-reducing bacteria from a diversity of environments. *Appl. Environ. Microbiol.* **64**: 1504–1509.

- CORNELL, R. M., AND U. SCHWERTMANN. 1996. The iron oxides. VCH.
- DAVISON, W. 1993. Iron and manganese in lakes. *Earth Sci. Rev.* **34**: 119–163.
- FRENZEL, P., U. BOSSE, AND P. H. JANSSEN. 1999. Rice roots and methanogenesis in a paddy soil: Ferric iron as an alternative electron acceptor in the rooted soil. *Soil Biol. Biochem.* **31**: 421–430.
- GHIORSE, W. C. 1988. Microbial reduction of manganese and iron, p. 305–331. *In* A. J. B. Zehnder [ed], *Biology of anaerobic microorganisms*. Wiley.
- GIBSON, G. R., R. J. PARKES, AND R. A. HERBERT. 1987. Evaluation of viable counting procedures for the enumeration of sulfate-reducing bacteria in estuarine sediments. *J. Microbiol. Methods* **7**: 201–210.
- HERING, J. G., AND W. STUMM. 1990. Oxidative and reductive dissolution of minerals, p. 427–464. *In* M. F. Hochella and A. F. White [eds.], *Mineral-water interface geochemistry*. Mineralogical Society of America.
- HINES, M. E., J. FAGANELI, AND R. PLANINC. 1997. Sedimentary anaerobic microbial biogeochemistry in the Gulf of Trieste, northern Adriatic Sea: Influences of bottom water oxygen depletion. *Biogeochemistry* **39**: 65–86.
- IMSL. 1997. IMSL Fortran subroutines for statistical applications, stat/library, vol. 1. Visual Numerics.
- JORGENSEN, B. B. 1978. A comparison of methods for the quantification of bacterial sulfate reduction in coastal marine sediments I. Measurement with radiotracer techniques. *Geomicrobiol. J.* **1**: 11–28.
- JUGSUIJNDA, A., R. D. DELAUNE, AND W. H. PATRICK. 1987. A comparison of microbially and chemically reducible iron in three soils. *Plant Soil* **103**: 281–284.
- LARSEN, O., AND D. POSTMA. 2001. Kinetics of reductive bulk dissolution of lepidocrocite, ferrihydrite, and goethite. *Geochim. Cosmochim. Acta* **65**: 1367–1379.
- LOVLEY, D. R. 1987. Organic matter mineralization with the reduction of ferric iron: A review. *Geomicrobiol. J.* **5**: 375–399.
- . 1991. Dissimilatory Fe(III) and Mn(IV) reduction. *Microbiol. Rev.* **55**: 259–287.
- . 2000. Fe(III) and Mn(IV) reduction, p. 3–30. *In* D. R. Lovley [ed.], *Environmental metal-microbe interactions*. ASM.
- , J. D. COATES, E. L. BLUNT-HARRIS, E. J. P. PHILLIPS, AND J. C. WOODWARD. 1996. Humic substances as electron acceptors for microbial respiration. *Nature* **382**: 445–448.
- , J. L. FRAGA, E. L. BLUNT-HARRIS, L. A. HAYES, E. J. P. PHILLIPS, AND J. D. COATES. 1998. Humic substances as a mediator for microbially catalyzed metal reduction. *Acta Hydrochim. Hydrobiol.* **26**: 152–157.
- , AND E. J. P. PHILLIPS. 1986a. Availability of ferric iron for microbial reduction in bottom sediments of the freshwater tidal Potomac River. *Appl. Environ. Microbiol.* **52**: 751–757.
- , AND ———. 1986b. Organic matter mineralization with reduction of ferric iron in anaerobic sediments. *Appl. Environ. Microbiol.* **51**: 683–689.
- , AND ———. 1987. Rapid assay for microbially reducible ferric iron in aquatic sediments. *Appl. Environ. Microbiol.* **53**: 1536–1540.
- , AND J. C. WOODWARD. 1996. Mechanisms for chelator stimulation of microbial Fe(III) oxide reduction. *Chem. Geol.* **132**: 19–24.
- MANN, C. J., AND R. G. WETZEL. 2000. Hydrology of an impounded lotic wetland—wetland sediment characteristics. *Wetlands* **20**: 23–32.
- NEVIN, K., AND D. R. LOVLEY. *In press*. Mechanisms of Fe(III) oxide reduction in sedimentary environments. *Geomicrobiol. J.*
- PONNAMPERUMA, F. N. 1972. The chemistry of submerged soils. *Adv. Agron.* **24**: 29–96.
- POSTMA, D. 1993. The reactivity of iron oxides in sediments: A kinetic approach. *Geochim. Cosmochim. Acta* **57**: 5027–5034.
- RAMSING, N. R., H. FOSSING, T. G. FERDELMAN, F. ANDERSEN, AND B. THAMDRUP. 1996. Distribution of bacterial populations in a stratified fjord (Mariager Fjord, Denmark) quantified by in situ hybridization and related to chemical gradients in the water column. *Appl. Environ. Microbiol.* **62**: 1391–1404.
- RITTMAN, B. E., AND J. M. VAN BRIESEN. 1996. Microbiological processes in reactive transport modeling, p. 311–334. *In* P. C. Lichtner, C. I. Steefel, and E. H. Oelkers [eds.], *Reactive transport in porous media*. The Mineralogical Society of America.
- RODÉN, E. E., AND J. W. EDMONDS. 1997. Phosphate mobilization in iron-rich anaerobic sediments: Microbial Fe(III) oxide reduction versus iron-sulfide formation. *Arch. Hydrobiol.* **139**: 347–378.
- , AND D. R. LOVLEY. 1993. Evaluation of ^{55}Fe as a tracer of Fe(III) reduction in aquatic sediments. *Geomicrobiol. J.* **11**: 49–56.
- , AND M. M. URRUTIA. 1999. Ferrous iron removal promotes microbial reduction of crystalline iron(III) oxides. *Environ. Sci. Technol.* **33**: 1847–1853.
- , ———, AND C. J. MANN. 2000. Bacterial reductive dissolution of crystalline Fe(III) oxide in continuous-flow column reactors. *Appl. Environ. Microbiol.* **66**: 1062–1065.
- , AND R. G. WETZEL. 1996. Organic carbon oxidation and suppression of methane production by microbial Fe(III) oxide reduction in vegetated and unvegetated freshwater wetland sediments. *Limnol. Oceanogr.* **41**: 1733–1748.
- , AND J. M. ZACHARA. 1996. Microbial reduction of crystalline iron(III) oxides: Influence of oxide surface area and potential for cell growth. *Environ. Sci. Technol.* **30**: 1618–1628.
- ROONEY-VARGA, J. N., R. T. ANDERSON, J. L. FRAGA, D. RINGELBERG, AND D. R. LOVLEY. 1999. Microbial communities associated with anaerobic benzene degradation in a petroleum-contaminated aquifer. *Appl. Environ. Microbiol.* **65**: 3056–3063.
- SNOEYENBOS-WEST, O. L., K. P. NEVIN, R. T. ANDERSON, AND D. R. LOVLEY. 2000. Enrichment of *Geobacter* species in response to stimulation of Fe(III) reduction in sandy aquifer sediments. *Microb. Ecol.* **39**: 153–167.
- STANLEY, E. H., AND A. K. WARD. 1997. Inorganic nitrogen regimes in an Alabama wetland. *J. N. Am. Benthol. Soc.* **16**: 820–832.
- STUMM, W. 1992. *Chemistry of the solid-water interface*. Wiley.
- , AND J. J. MORGAN. 1996. *Aquatic chemistry*. Wiley.
- , AND B. SULZBERGER. 1992. The cycling of iron in natural environments: Considerations based on laboratory studies of heterogeneous redox processes. *Geochim. Cosmochim. Acta* **56**: 3233–3257.
- SULZBERGER, B., D. SUTER, C. SIFFERT, S. BANWART, AND W. STUMM. 1989. Dissolution of Fe(III) (hydr)oxides in natural waters: Laboratory assessment on the kinetics controlled by surface coordination. *Mar. Chem.* **28**: 127–144.
- SUTER, D., S. BANWART, AND W. STUMM. 1991. Dissolution of hydrous iron(III) oxides by reductive mechanisms. *Langmuir* **7**: 809–813.
- THAMDRUP, B. 2000. Bacterial manganese and iron reduction in aquatic sediments. *Adv. Microb. Ecol.* **16**: 41–84.
- , H. FOSSING, AND B. B. JORGENSEN. 1994. Manganese, iron, and sulfur cycling in a coastal marine sediment, Aarhus Bay, Denmark. *Geochim. Cosmochim. Acta* **58**: 5115–5129.
- URRUTIA, M. M., E. E. RODÉN, J. K. FREDRICKSON, AND J. M. ZACHARA. 1998. Microbial and geochemical controls on syn-

- thetic Fe(III) oxide reduction by *Shewanella alga* strain BrY. *Geomicrobiol. J.* **15**: 269–291.
- , ———, AND J. M. ZACHARA. 1999. Influence of aqueous and solid-phase Fe(II) complexants on microbial reduction of crystalline Fe(III) oxides. *Environ. Sci. Technol.* **33**: 4022–4028.
- VAN BODEGOM, P. M., AND J. C. M. SCHOLTEN. 2001. Microbial processes of CH₄ production in a rice paddy soil: Model and experimental validation. *Geochim. Cosmochim. Acta.* **65**: 2055–2066.
- VAN CAPPELLEN, P., AND Y. WANG. 1995. Metal cycling in surface sediments: Modeling the interplay of transport and reaction, p. 21–64. *In* H. E. Allen [ed.], *Metal contaminated aquatic sediments*. Ann Arbor Press.
- , AND ———. 1996. Cycling of iron and manganese in surface sediments: A general theory for the coupled transport and reaction of carbon, oxygen, nitrogen, sulfur, iron, and manganese. *Am. J. Sci.* **296**: 197–243.
- VAN DER NAT, F. W. A., AND J. J. MIDDELBURG. 1998. Effects of two common macrophytes on methane dynamics in freshwater sediments. *Biogeochemistry* **41**: 1–22.
- VESTER, F., AND K. INVORSEN. 1998. Improved most-probable-number method to detect sulfate-reducing bacteria with natural media and a radiotracer. *Appl. Environ. Microbiol.* **64**: 1700–1707.
- WALLMANN, K., K. HENNIES, I. KONIG, W. PETERSEN, AND H. D. KNAUTH. 1993. New procedure for determining reactive Fe(III) and Fe(II) minerals in sediments. *Limnol. Oceanogr.* **38**: 1803–1812.
- WESTRICH, J. T., AND R. A. BERNER. 1984. The role of sedimentary organic matter in bacterial sulfate reduction: The G model tested. *Limnol. Oceanogr.* **29**: 236–249.
- WOOMER, P. L. 1994. Most probable number counts, p. 59–79. *In* J. M. Bigham [ed.], *Methods of soil analysis Part 2—Microbiological and biochemical properties*. Soil Science Society of America.
- ZACHARA, J. M., J. K. FREDRICKSON, S. W. LI, D. W. KENNEDY, S. C. SMITH, AND P. L. GASSMAN. 1998. Bacterial reduction of crystalline Fe(III) oxides in single phase suspensions and subsurface materials. *Am. Mineral.* **83**: 1426–1443.

Received: 6 April 2001

Accepted: 24 August 2001

Amended: 17 September 2001